

Microlens Mass Functions

William D. Heacox

November 15, 2018

Abstract

A non-parametric statistical model is constructed to directly relate the distribution of observed microlens timescales to that of the mass function of the population from which the lenses are drawn, corrected for observational selection based on timescales and event amplifications. Explicit distributions are derived for microlensing impact parameters and maximum amplifications; both are shown to be statistically independent of all other parameters in the problem, including lens mass. The model is used to demonstrate that the narrow range of microlens timescales observed toward the Large Magellanic Cloud (LMC) is probably not consistent with lensing by a widely distributed spheroidal population (“dark halo”) of large velocity dispersion, but is consistent with lensing within a rotating thick disk. Poor numerical conditioning of the statistical connection between lens masses and event timescales, and small number statistics, severely limit the mass function information obtainable from current microlensing surveys toward the LMC.

1 INTRODUCTION

Microlensing is a promising tool for eliciting the properties of massive compact objects in the Galactic halo and toward the Galactic bulge, and several such observing programs are underway or have been completed. In particular, the MACHO and EROS projects have published results for several years of monitoring $> 10^6$ stars in the Large Magellanic Cloud (LMC; Alcock et al. 2000, Milsztajn et al. 2001), which detected 10–20 events; and both the MACHO and OGLE projects (Udalski et al. 2000) have published the results of microlensing surveys toward the Galactic bulge that include more than 200 events. Several additional microlensing surveys are currently underway. The results of these surveys have provided otherwise inaccessible information on the structure and contents of the Galaxy, but not always in unambiguous ways. The primary object of interest has been the total mass in the form of compact objects, particularly in the (presumably dark) Galactic halo, usually analyzed in the form of microlensing optical depths originally proposed by Paczyński (1986). As useful as these analyses have been, little information on the mass function of the population underlying the microlensing observations has been forthcoming, although

some parametric modeling (e.g., Green 2000) has sufficed to indicate some possible constraints conditional upon various kinematic models of the halo. Here we propose a more direct way to elucidate the mass function of the population responsible for microlenses, in the form of a non-parametric statistical model that directly relates the mass function to the microlens quantities being observed. In principle, such a model should allow an unambiguous determination of the mass function, given only the kinematics of the population. In practice, we expect that the information obtainable from such a method will be limited by small number statistics and ambiguities concerning the kinematics of the lensing population.

The necessary microlens physical relations are as follows (see, e.g., Paczyński 1996 or Gould 1996 for more complete discussions). The physical scale of a microlensing event in the lens plane (i.e., the plane of the sky at the lens location) is given by the Einstein radius:

$$r_E = \frac{2}{c} \sqrt{\frac{GM D_L (D_S - D_L)}{D_S}}, \quad (1)$$

where D_L and D_S are, respectively, lens and source star distances from the observer; and M is the lens mass. For solar-mass halo microlenses viewed against the backdrop of the LMC, r_E is typically a few astronomical units. In terms of this quantity, the scaled impact parameter β and event timescale \mathcal{T} are defined to be

$$\beta = b/r_E, \quad (2)$$

$$\mathcal{T} = r_E/V_\perp, \quad (3)$$

where b , the ‘‘impact parameter’’, is the closest approach to the lens of the line-of-sight to the source star and V_\perp is the relative transverse velocity of the encounter, both measured in the lens plane. The maximum optical amplification of the event is

$$\mathcal{A} = \frac{\beta^2 + 2}{\beta\sqrt{\beta^2 + 4}} \Rightarrow \beta(\mathcal{A}) = \left[2 \left(\frac{\mathcal{A}}{\sqrt{\mathcal{A}^2 - 1}} - 1 \right) \right]^{1/2}. \quad (4)$$

The quantities \mathcal{A} and \mathcal{T} are easily derived from the event light curve, and constitute the physically significant observables for simple (i.e., point-source and point-lens) microlenses.

Within a homogeneous set of observed microlenses, the overall statistical distribution of observables, $f_{\mathcal{A},\mathcal{T}}(\mathcal{A},\mathcal{T})$, can be formally related to that of lens mass among the population from which they were drawn, $f_M(M)$, by a relation of the form

$$f_{\mathcal{A},\mathcal{T}}(\mathcal{A},\mathcal{T}) = \int f_{\mathcal{A},\mathcal{T}|M}(\mathcal{A},\mathcal{T}|M) f_M(M) dM. \quad (5)$$

The notation is that $f_x(y)$ is the probability density function (pdf) of random variable x evaluated at $x = y$; $f_{x|z}$ is the pdf of x conditional upon z . The

core of the model is the kernel function $f_{\mathcal{A},\mathcal{T}|M}(\mathcal{A},\mathcal{T}|M)$, the probability that an object of mass M will yield a microlensing event characterized by $(\mathcal{A},\mathcal{T})$. This is essentially an accounting mechanism, one that adds up the probabilities of all possible combinations of lensing parameters (b, V_{\perp}, D_L, D_S) that lead to the observed $(\mathcal{A},\mathcal{T})$, given mass M . Its computation requires the provision of a kinematic model of the lens and source populations; i.e., *a priori* distributions of (b, V_{\perp}, D_L, D_S) . Having computed the kernel, one numerically inverts the statistical model (eq. [5]) in terms of the observed $f_{\mathcal{A},\mathcal{T}}$ to determine the desired mass function characterizing the population producing the microlenses. With kinematically well-characterized populations – e.g., those (presumably) of the Galactic halo and LMC – this procedure appears to be a reasonable one for estimating the mass function of the lensing population.

2 STATISTICAL MODEL

2.1 Derivation

The detailed statistical relation can be derived as follows. Starting from the marginalization tautology

$$f_{\mathcal{A},\mathcal{T}}(\mathcal{A},\mathcal{T}) = \int \int \int f_{\mathcal{A},\mathcal{T},D_L,D_S,M}(\mathcal{A},\mathcal{T},D_L,D_S,M) dD_L dD_S dM, \quad (6)$$

one changes variables within the integrand, from \mathcal{A} and \mathcal{T} to $b = r_E \beta(\mathcal{A})$ and $V_{\perp} = r_E/\mathcal{T}$:

$$f_{\mathcal{A},\mathcal{T}}(\mathcal{A},\mathcal{T}) = \int \int \int f_b(r_E \beta(\mathcal{A})) f_{V_{\perp},D_L,D_S,M}\left(\frac{r_E}{\mathcal{T}}, D_L, D_S, M\right) |\mathbf{J}| dD_L dD_S dM. \quad (7)$$

As shown in Appendix A, in any likely application the impact parameter b will be uniformly distributed independently of any other parameters, so that its distribution f_b may be factored away from that of the other parameters and assumed to be a constant that can be absorbed into normalization of the model. The quantity $|\mathbf{J}|$ is the Jacobian of the variable transformation:

$$|\mathbf{J}| = \left| \begin{array}{cc} \partial b/\partial \mathcal{A} & \partial b/\partial \mathcal{T} \\ \partial V_{\perp}/\partial \mathcal{A} & \partial V_{\perp}/\partial \mathcal{T} \end{array} \right| = \frac{r_E^2}{\mathcal{T}^2} \left[2 \left(\frac{\mathcal{A}}{\sqrt{\mathcal{A}^2 - 1}} - 1 \right) (\mathcal{A}^2 - 1)^3 \right]^{-1/2}. \quad (8)$$

Combining these results,

$$f_{\mathcal{A},\mathcal{T}}(\mathcal{A},\mathcal{T}) = C \frac{L_{\mathcal{A}}(\mathcal{A})}{\mathcal{T}^2} \int \int \int r_E^2 f_{V_{\perp},D_L,D_S,M}\left(\frac{r_E}{\mathcal{T}}, D_L, D_S, M\right) dD_L dD_S dM, \quad (9)$$

where C is a constant and all of the amplitude information is contained within the likelihood function

$$L_{\mathcal{A}}(\mathcal{A}) = \left[\left(\frac{\mathcal{A}}{\sqrt{\mathcal{A}^2 - 1}} - 1 \right) (\mathcal{A}^2 - 1)^3 \right]^{-1/2}, \quad (10)$$

which is independent of any other parameters in the problem. Equation (9) makes clear that \mathcal{A} and M are effectively statistically independent, so the lensing amplitude carries no significant mass information. We can thus treat \mathcal{A} as a nuisance parameter and integrate it from the model, leaving one in which the only observable information is that of timescale \mathcal{T} . The integral of $L_{\mathcal{A}}$ actually diverges as $\mathcal{A} \rightarrow 1$, but that lower limit corresponds to unobservably faint microlenses: in any practical observing program there will be a minimum observable amplitude, however poorly defined, that serves to determine the value of the integral of equation (9) over \mathcal{A} , and to partly convert the left-hand side of that equation to one of observed microlenses. To complete that conversion, we multiply the model by the probability $E(\mathcal{T})$ that a microlens of timescale \mathcal{T} will actually be observed; this may be estimated by the observer based on properties of the observing process, so the (non-normalized) model becomes one corrected for observational selection:

$$f_{\mathcal{T}}^{(O)}(\mathcal{T}) \propto \frac{E(\mathcal{T})}{\mathcal{T}^2} \int \int \int r_E^2 f_{V_{\perp}, D_L, D_S, M}^{(P)}\left(\frac{r_E}{\mathcal{T}}, D_L, D_S, M\right) dD_L dD_S dM . \quad (11)$$

The superscript (O) on the observable $f_{\mathcal{T}}$ denotes a distribution of observed lenses only, while the (P) on the integrand refers to the distribution among the entire population of objects from which the observed lenses and sources are drawn.

Put nearly into the standard form of equation 5, we have

$$f_{\mathcal{T}}^{(O)}(\mathcal{T}) = C \int L_{\mathcal{T}|M}(\mathcal{T}|M) f_M^{(P)}(M) dM , \quad (12)$$

where

$$L_{\mathcal{T}|M}(\mathcal{T}|M) = \frac{E(\mathcal{T})}{\mathcal{T}^2} \int \int r_E^2 f_{V_{\perp}, D_L, D_S|M}^{(P)}\left(\frac{r_E}{\mathcal{T}}, D_L, D_S|M\right) dD_L dD_S \quad (13)$$

is the likelihood of observing a microlens of timescale \mathcal{T} arising from a lensing object of mass M (which enters via r_E ; cf. eq. [1]). This – equations 12 and 13 – is the desired result, the deterministic connection between lens population mass function and observed timescale distribution (the normalizing factor C is to be computed *a posteriori* from normalization of $f_{\mathcal{T}}^{(O)}(\mathcal{T})$).

2.2 A Corroborating Example

As an example loosely based on observations of microlenses toward the LMC, we postulate a thick disk whose stellar spatial density varies along the line-of-sight to the LMC as $\rho(D) \propto \exp(-D/l)$, where $l = 8$ kpc is the projected scale length. From Appendix C we then expect the linear distribution of stellar distances to be $f_{D_L}(D_L) \propto D_L^2 \exp(-D/l)$. We also postulate a Maxwellian velocity distribution for V_{\perp} of 200 km s⁻¹ rms, and put all the source stars at $D_S = 55$ kpc. Assuming statistical independence of D_L , D_S , V_{\perp} , and M ; and a timescale observing efficiency of $E(\mathcal{T}) = \mathcal{T}(200 - \mathcal{T})$ for $0 \leq \mathcal{T} \leq 200$ days and

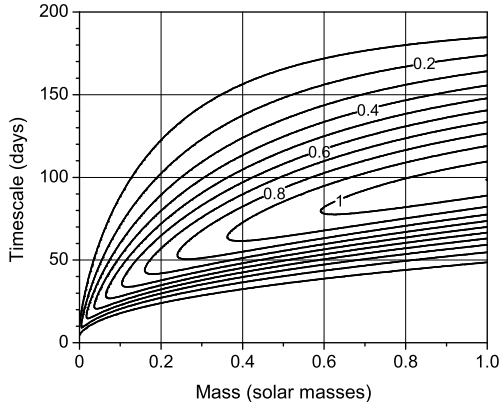


Figure 1: Relative likelihood $L_{\mathcal{T}|M}(\mathcal{T}|M)$ (eq. [13], arbitrarily scaled) that a compact object of mass M will produce an observable microlensing event of timescale \mathcal{T} , for a synthetic kinematic model and timescale observing efficiency (see text).

0 otherwise; we use equation 13 to compute the integral kernel shown in Figure 1. With a presumed lensing population mass function uniform on $(0, 1)$ solar masses, this kernel yields (from eq. [12]) the timescale distribution of observable microlenses shown in Figure 2. Also shown in this figure are the corroborating results of one of many Monte Carlo simulations with sample lensing object kinematics drawn directly from the above distributions, without reference to the statistical model (the simulations employed $b_{\max} = 20$ A.U. (Appendix A) and $\mathcal{A}_{\min} = 1.3$ for observable lenses, neither of which affects the results; and employs the same $E(\mathcal{T})$ as used in the model). The excellent agreement between model predictions and an independent simulation suggests an accurate model, fully corrected for timescale- and amplitude-limited observational selection.

2.3 Solution

The model may be numerically inverted to determine the underlying population mass function from an observed timescale distribution. The simplest inversion technique may be that of Richardson (1972) and Lucy (1974), in the form proposed by Heacock (1997, eq. [A4]). Suppressing the (P) and (O) superscripts for clarity, this iterative algorithm takes the form

$$\mathcal{L}^{(n)}(\mathcal{T}, M) = \frac{L_{\mathcal{T}|M}(\mathcal{T}|M)}{\int L_{\mathcal{T}|M}(t|m) f_M^{(n)}(m) dm dt}, \quad (14)$$

$$f_M^{(n+1)}(M) = f_M^{(n)}(M) \int \frac{\mathcal{L}^{(n)}(t, M) f_{\mathcal{T}}(t)}{\int \mathcal{L}^{(n)}(t, m) f_M^{(n)}(m) dm} dt. \quad (15)$$

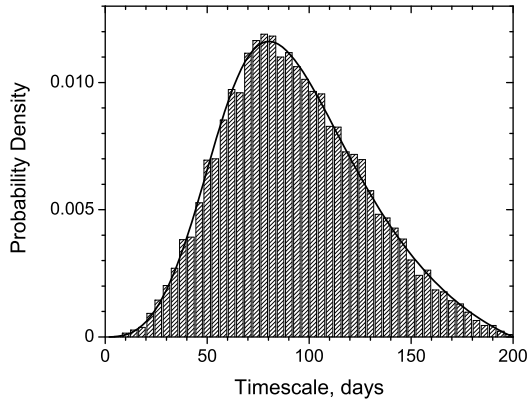


Figure 2: Timescale distribution $f_{\mathcal{T}}(\mathcal{T})$ for a hypothetical lensing population kinematic model and uniform mass function (see text). Solid curve: as predicted by the statistical model and computed from the kernel function of Figure 1 and adopted mass function. Histogram: as simulated by Monte Carlo sampling from the presumed kinematic distributions and mass function, without reference to the statistical model.

One chooses an initial guess for $f_M^{(1)}(M)$ (prudently chosen to be smooth on a wide range) and iterates until sensible convergence. If the observed $f_{\mathcal{T}}^{(O)}$ is actually derived from the presumed kinematic model, the method will almost always converge to a reasonable approximation to the underlying mass function. Note, however, that the statistical model is a smooth, non-linear mapping from the space of mass functions into that of observed timescale functions, for which we do not expect that every timescale distribution will have a legitimate mass function pre-image, given the adopted kinematic model. If either the timescale function is inaccurate (due, e.g., to sampling variations) or the adopted kinematic model is incorrect, the Richardson-Lucy method may fail to converge when applied to this statistical model.

3 APPLICATION TO GALACTIC HALO MICROLENSSES

3.1 Data

The lensing population responsible for microlenses observed against the backdrop of the LMC probably represents the kinematically most homogeneous set of objects to be analyzed for mass function with the statistical model of the previous section. The MACHO Project (Alcock et al. 2000) has detected between 13 (Criteria A) and 17 (Criteria B) “simple” (point-source and point-mass) lensing events over a 5.7-year period. The timescale ((T)) distributions for these

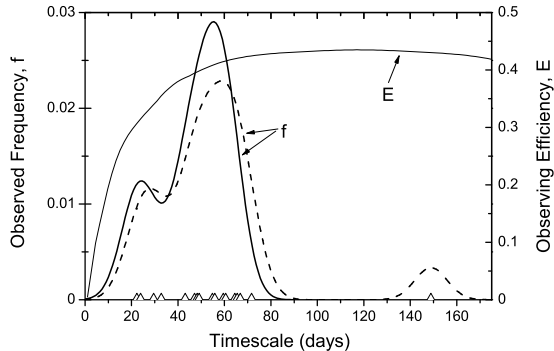


Figure 3: Observed microlens timescale distribution toward the LMC. Solid, heavy curve: Alcock et al.’s (2000) high-confidence events (“Criteria A”); dashed curve, lower-confidence events (“Criteria B”). Light curve: estimated timescale observability (a transcription of Alcock et al.’s (2002) 5-year Criteria A curve of their Figure 5). The symbols at the bottom denote the timescales for individual Criteria B events (those of Criteria A are an approximate subset).

observations are shown in Figure 3, together with their estimated observing efficiency $E(\mathcal{T})$ (note that the timescale \hat{t} of Alcock et al. (2000) is $2\mathcal{T}$).

The timescale frequency functions as shown are Gaussian kernel estimators applied to Alcock et al.’s (2000) individual events (their Table 7), with a smoothing kernel standard deviation set as large as possible (7 days) consistent with the very low estimated probability of detecting events with timescales less than ~ 2 days. The multi-modality of these distributions is quite possibly an artifact of small sample statistics, but the narrow range of observed timescales probably is not (the matter is discussed further in §4).

3.2 Kinematic Model

There appears to be no unambiguous kinematic model of the dark halo with which these data may be used in application of the statistical model. While there is some dynamical evidence for the dark halo mass distribution, there are few observational clues to the required velocity field even in the luminous halo. The root of the difficulty is that the velocity of interest here – that on the plane of the sky – is unobservable beyond the solar vicinity and cannot be reasonably inferred from equilibrium dynamical models based on the collisionless Boltzmann equation (Binney & Tremaine 1987). Beyond the solar vicinity, such velocities are largely transverse to the Galactic center and thus reflect orbital angular momentum as much as they do orbital energy. But angular momentum is essentially a free parameter in static equilibrium models, so that a whole sequence of models of different orbital angular momentum content may be fit to observed spatial densities and radial velocity distributions (Heggie & Hut 2003),

and there is thus no effective theoretical or observational constraint on halo transverse velocity distributions. Some evolutionary models of the luminous halo (e.g., Sommer-Larson et al. 1997) are consistent with reasonable levels of velocity anisotropy that, in conjunction with the observed radial velocity dispersion of distant halo stars, suggest a large ($> 100 \text{ km s}^{-1}$) transverse velocity dispersion throughout the halo. But it is not at all clear that such speculative dynamical models of the luminous halo can be confidently applied to the dark halo.

One is thus reduced to examining the compatibility of presumed dark halo kinematic models with the observed microlens timescale distribution. The initial choice of kinematic model has here been made so that all parameters are statistically independent (the alternative will be considered shortly) and with the narrow range of observed timescales in mind, so that the ranges of distances and velocities in the kinematic model have been kept as small as is reasonably consistent with a spheroidal, pressure-supported halo. Thus, the ‘‘NFW Law’’ of dark halo spatial mass density, $\rho(R) \propto R^{-1}(a+R)^{-2}$ (Navarro, Frank & White 1997), is chosen as the basis of the MACHO distance distribution, where R is the galactocentric distance and $a = 5 \text{ kpc}$ is the core radius. The resulting solarcentric distance distribution is then (from Appendix C):

$$f_{D_L}(D_L) \propto D_L^2 \left\{ R(D_L) [a + R(D_L)]^2 \right\}^{-1}, \quad (16)$$

where $R(D) = [D^2 + R_\odot^2 - 2DR_\odot \cos b_{LMC} \cos l_{LMC}]^{1/2}$ with $R_\odot = 8 \text{ kpc}$ presumed. LMC source star distances are taken to all be 55 kpc (the more realistic assumption of a depth to the LMC does not change the result). The transverse velocity V_\perp of the lens relative to the source, as seen from our location, includes the motion of the Sun relative to the LMC, and of the non-rotating halo rest frame relative to the Sun. The first of these is computed from the observed LMC proper motions of $\mu_{\alpha,\delta} = 1.20, 0.26$ micro-arcseconds per year (Jones, Klemola & Lin 1994) and an LMC distance of 55 kpc , the second from a presumed rotation rate of the Sun relative to the Halo of 200 km s^{-1} . The resulting mean velocity of the halo across the line-of-sight to the LMC is thus $\langle V \rangle = 215 \text{ km s}^{-1}$. Relative to this mean frame we conservatively adopt a halo velocity dispersion on the plane of the sky of 120 km s^{-1} (Binney & Merrifield 1998, Scheffler & Elsässer 1988, Sommer-Larsen et al. 1997) and realize this with low angular momentum orbits characterized by a dark halo internal Gaussian random velocity distribution of mean 0. With these and the presumption of no significant LMC internal velocities, we compute (by the method of §3 of Appendix B) the distribution of V_\perp shown in Figure 4.

3.3 Mass Function

The integral kernel $L_{\mathcal{T}|M}(\mathcal{T}|M)$ computed for these distributions (and assuming the $E(\mathcal{T})$ estimated by Alcock et al. 2000 and illustrated in Figure 3) is similar in appearance to that of the example shown in Figure 1. In application to

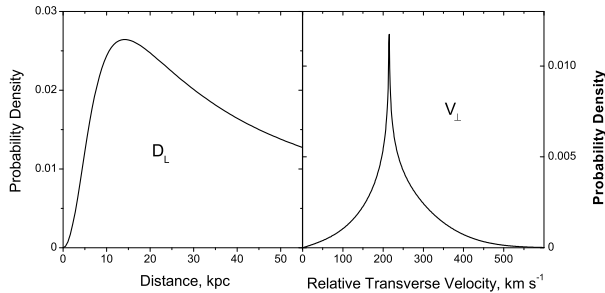


Figure 4: Distributions of lens solarcentric distances D_L (left panel) and relative transverse velocities V_{\perp} (right panel) in the assumed dark halo kinematic model (see text).

presumptive lens populations of a single mass (i.e., $f_M(M)$ as a delta function centered on the chosen mass), this model gives rise to the sample timescale distributions shown in Figure 5.

It is apparent that no non-pathological lens mass function can adequately reproduce the observed timescale distribution, given this kinematic model (the Richardson-Lucy interactive inversion method of §2.3, applied to this model and Alcock et al.’s [2000] Criteria A observed timescale function, does not converge). The difficulty can be ascribed to the wide range of lens distances and velocities in the kinematic model, which lead to similarly wide ranges of observed timescales for given lens mass.

The obvious alternative kinematic models do little, if anything, to rectify this discrepancy. Isothermal models, both with and without mass segregation, lead to different kernels $L_{\mathcal{T}|M}(\mathcal{T}|M)$ but similarly widely distributed timescale distributions irrespective of lens mass. A choice of different dark halo mass distribution (e.g., $\rho(R) \propto (a^2 + R^2)^{-1}$ or $(a + R)^{-2}$; Binney & Merrifield 1998, Alcock et al. 1996, 1997) will typically exacerbate the problem, as will the inclusion of LMC internal velocity dispersion in the computation of V_{\perp} . The timescale distribution widths may only be adequately decreased in a spheroidal halo by (1) postulating a halo velocity field with a very small transverse velocity dispersion, probably less than $\sim 50 \text{ km s}^{-1}$, while continuing to ignore the LMC internal motions; and/or (2) greatly decreasing the spatial range encompassed by the lensing populations, as in a thin shell. Neither of these seems dynamically plausible. Additional caveats, based on the small sample size and poor numerical conditioning of the statistical model, are discussed in §4. For the moment, the microlens timescale distribution as observed appears to be inconsistent with a standard, spheroidal, pressure-supported model of the dark halo.

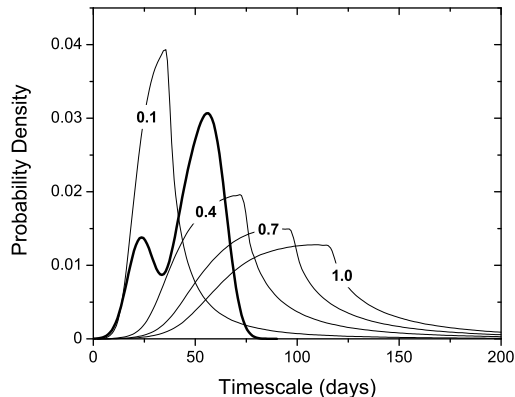


Figure 5: Microlens time scale distributions (light curves) predicted for single-mass lensing populations from a spheroidal, pressure-supported, low angular momentum kinematic model of the halo (see text). The distributions are labeled with the stellar mass (solar masses) that produced them. The heavy curve is the adopted observed timescale distribution (Criteria A of Alcock et al. 2000).

3.4 Thick Disk Model

As one possible alternative to the dark halo microlensing model we consider a rotating, low-dispersion, thick disk as the site of microlensing objects. To be consistent with the roughly constant rotation velocity in the outer disk, we adopt a spatial mass density that varies with galactocentric distance r in the disk, and height z above the disk, of $\rho(r, h) \propto r^{-1} \exp(-z/h)$. Following the argument of Appendix C, the distribution of solarcentric distances will be

$$f_{D_L}(D_L) \propto D_L^2 r(D_L)^{-1} \exp\left[-\frac{D_L \sin|b_{LMC}|}{h}\right], \quad (17)$$

where $r(D) = [D^2 \cos^2 b_{LMC} + R_\odot^2 - 2DR_\odot \cos b_{LMC} \cos l_{LMC}]^{1/2}$ and we again choose $R_\odot = 8$ kpc. To keep the timescale dispersions small we choose $h = 2$ kpc in a co-rotating thick disk of 30 km s^{-1} velocity dispersion. Both of these are at the low end of what would be expected, both observationally and dynamically; but they seem possible. We further assume the statistical independence of all kinematic parameters, a constant source distance of 55 kpc, and an internal velocity dispersion of 30 km s^{-1} for the LMC (but no rotation). Then the integral kernel $L_{\mathcal{T}|M}(\mathcal{T}|M)$ corresponding to this kinematic model produces the single-mass timescale functions of Figure 6, from which it is apparent that a distribution of lens masses encompassing roughly 0.1 to 0.7 solar masses may suffice to explain the MACHO observed timescale distribution. In this case the Richardson-Lucy inversion procedure of §2.3 converges to the results shown in Figure 7. For this postulated thick disk there is no evidence for lensing objects

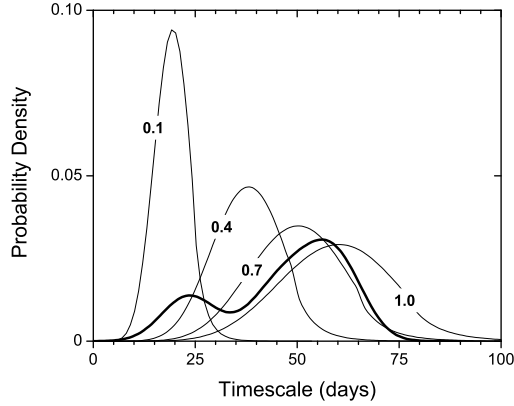


Figure 6: As with Figure 5, but for a rotating, low velocity dispersion, thick disk population (see text). The thin curves are labeled with the lens mass (solar masses); the thick curve is the MACHO observed timescale distribution (Alcock et al. 2000).

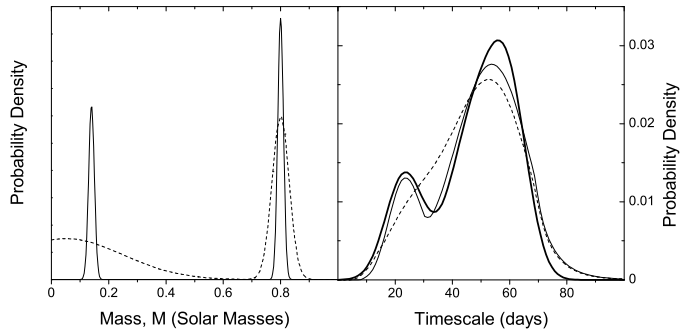


Figure 7: Thick disk mass functions approximate solutions. Left panel: mass functions (arbitrarily scaled) inferred from the Richardson-Lucy algorithm applied to the statistical model derived from an adopted thick disk kinematic model (see text) and observed timescale function (solid curve of Figure 3). Solid curve: 200 interactions beginning from a uniform mass distribution. Dashed curve: 100 interactions. Right panel: the timescale distributions (light curves) corresponding to the mass functions in the left panel, as computed from the statistical model (eq. [12] and 13). The heavy curve is the observed timescale distribution.

exceeding one solar mass, and some evidence that a significant fraction of the lenses have low- or sub-stellar masses.

4 SUMMARY AND CONCLUSIONS

The statistical model of equations 12 and 13 is the complete deterministic connection between the lens population mass function and the distribution of timescales among observed microlenses. It is fully corrected for observational selection based on timescale and maximum amplitude observability, providing these are mutually independent (which will usually be the case). The correction for selection on the basis of amplitude arises from a basic model (eq. [9]) that includes the amplitude as an observable, from which it is removed by integration over, in effect, observable amplitudes only. The result (easily proven by construction of a basic model for timescales only) is the inclusion of an additional factor of r_E in the integrand: the observability of a microlensing event, in terms only of amplitude, is proportional to the Einstein radius of the lens, hence (approximately) to $M^{1/2}$.

Appendix A provides a formal derivation of event impact parameter distributions: for all practical purposes these are uniform on a range exceeding that likely to be encountered in amplitude-limited observations. These results lead to a formal distribution of event amplitudes (eq. [10]), which is independent of kinematic model parameters and of lens mass; so that microlens mass information must come only from event timescales. These are both familiar results, here rigorously derived.

The statistical model is limited in applicability by its relatively poor numerical conditioning, reflective of the small contribution of lens mass to the event timescale. The formal concept of condition number is not strictly applicable to such non-linear models, but the sensitivity of the observed timescale distribution to the mass function can be crudely estimated as the change in mean timescale (as computed from the model) for a given change in scale of a mass delta function. For the example of §2.2, this sensitivity is about $\Delta \langle T \rangle \approx 7$ days per $\Delta M = 0.1$ solar masses over the range of (0.1, 1) solar masses. While this number depends upon the kinematic model adopted, it is probably typical of most applications to widely distributed kinematics and suggests a relatively poorly conditioned model from which mass function information will be difficult to extract.

The poor numerical conditioning of the model is reflected in its smoothing effect in translating mass functions into timescale distributions. This is apparent from the thick disk model result of §3.4, where nearly delta-function mass distributions serve to reproduce the smooth, bimodal observed timescale distribution. It is for this reason that no realistic mass function can reproduce the substantial timescale structure in Alcock et al.'s (2000) Criteria B sample (dashed curve in Figure 5): the isolated event near 150 days, if real, is a true outlier, perhaps arising from a separate lens population.

For microlensing toward the LMC, the conditioning difficulty is exacerbated

by uncertainties in the observed timescale distribution due to small sample statistics. Re-sampling of the presumed timescale distribution (Criteria A of Alcock et al. 2000; heavy curve in Figure 5) demonstrates that a wide range of timescale distributions is likely to arise from such a small sample. A significant fraction of 13-object distributions drawn from, e.g., a Gaussian of mean 50 days and standard deviation 15 days (roughly those of Criteria A events) show bimodality similar to that of the Criteria A distribution, so that the observed bi-modality may well be a spurious consequence of small-number statistics.

It thus seems unlikely that the current microlensing observations toward the LMC could meaningfully constrain the (presumably) underlying dark halo mass function. Even such summary statistics as the mean mass are in some doubt: since $M \propto V_{\perp}^2$ for given event timescale, and the mean of V_{\perp} depends as much upon the poorly known LMC proper motions as it does on the solar galactocentric velocity, the canonical value of $\langle M \rangle \approx 0.5$ solar mass (e.g., Alcock et al. 2000) may well be incorrect by a substantial factor.

But the narrow range of observed timescales appears to be real: re-sampling experiments from this and similar distributions suggest little likelihood that the true distribution is sufficiently broader than that observed as to be compatible with kinematic distributions as broadly distributed as those expected of a spheroidal, pressure-supported population of modest mean orbital angular momentum. It seems likely that the population producing the microlenses observed toward the LMC must come from something other than a “standard” halo, either dark or luminous. The results of §3.4 suggest that a thick disk origin is one possibility; no doubt there are others.

A IMPACT PARAMETER DISTRIBUTION

We take as the most likely geometric model one in which, at the commencement of the survey, the lensing candidates are uniformly distributed on the plane of the sky in the vicinity of the source star being observed. The geometry of the encounter is described entirely by the original distance between lensing object and source star, r , and the direction ξ of motion relative to the radius vector from star to lens; both measured in the lens plane. The impact parameter corresponding to (r, ξ) will then be $b = r \sin \xi$; r will be distributed as $f_r(r) = 2r/r_{\max}^2$ where r_{\max} is the limiting radius of the search area in the lens plane; and, by virtue of the uniform distribution of lens locations, we can safely presume ξ to be uniformly distributed on $(0, \pi/2)$. By a useful theorem of cumulative distributions (e.g., §7.26 of Kendall, Stuart and Ord 1987), the pdf of b is given by

$$f_b(b) = \frac{d}{db} \int_{\Omega} \int f_r(r) f_{\xi}(x) d\xi dr, \quad (18)$$

where $\Omega = \{(r, \xi) | r \sin \xi < b\}$ is the set of all lens coordinates for which the impact parameter is less than b . Thus:

$$f_b(b) = \frac{d}{db} \left[\int_0^b \int_0^{\pi/2} + \int_b^{r_{\max}} \int_0^{\arcsin(b/r)} \right] \left(\frac{4r}{\pi r_{\max}^2} \right) d\xi dr, \quad (19)$$

$$= \frac{4}{\pi r_{\max}} \left[1 - \left(\frac{b}{r_{\max}} \right)^2 \right]^{1/2}, \quad (20)$$

for $0 \leq b \leq r_{\max}$ and 0 otherwise. This formula has been verified by Monte Carlo simulations based on the above geometric model. In most applications the largest impact parameter corresponding to observable amplitudes will be smaller than r_{\max} by several orders of magnitude (about 6 – 10 for observable halo microlenses) and $f_b(b)$ may safely be taken to be a constant independent of all other parameters. The above result, with the assumption $b \ll r_{\max}$, leads to the amplitude likelihood of equation 10. From that relation the distribution of scaled impact parameter β is easily seen to be

$$f_{\beta}(\beta) \propto L_{\mathcal{A}}(\mathcal{A}(\beta)) \left| \frac{d\mathcal{A}}{d\beta} \right| = 1. \quad (21)$$

The distributions of observable microlens impact parameters, scaled or not, are thus expected to be uniform and independent of distributions of lens distances, velocities, or masses.

B VELOCITY DISTRIBUTIONS

The velocity V_{\perp} is the relative velocity of lens and source star, projected onto the plane of the sky, as seen from our location. It can usually be computed as the

magnitude of the vector sum of two or more projections of velocity components onto the plane of the sky. For many applications, the following results will suffice to compute the distribution of this quantity, from a kinematic model of the three-dimensional velocity distributions of lenses and source stars.

B.1 Projection onto Plane of Sky

An isotropic space velocity V will have a magnitude projected onto the plane of the sky, V_{pos} , given by the simple projection relation encountered in, e.g., analysis of binary star orbits (Chandresakhar and Münch 1950):

$$f_{V_{pos}}(V_{pos}) = V_{pos} \int_{V_{pos}}^{\infty} \frac{f_V(V)}{V \sqrt{V^2 - V_{pos}^2}} dV . \quad (22)$$

B.2 Combination of Random Velocities

Two statistically independent, mutually orthogonal, random velocity components (V_x, V_y) on the plane of the sky; have a combined magnitude $V = [V_x^2 + V_y^2]^{1/2}$ at a position angle $\theta = \arccos(V_x/V)$, whose joint distribution is given by the simple variable transformation:

$$f_{V,\theta}(V, \theta) = V f_{V_x}(V \sin \theta) f_{V_y}(V \cos \theta) \quad (23)$$

(V is the Jacobian). The marginal distribution of velocity magnitude alone is given by the integral of this expression over θ or, changing variables to $V_x = V \sin \theta$,

$$f_V(V) = V \int_0^V \frac{f_{V_x}(V_x) f_y(\sqrt{V^2 - V_x^2})}{\sqrt{V^2 - V_x^2}} dV_x . \quad (24)$$

B.3 Combination of Random & Streaming Velocities

The distribution of magnitudes of the combination of a random velocity V_R with a streaming velocity V_S (e.g., that arising from the LMC proper motions), both on the plane of the sky, may be computed as follows. Let $f_{V_R,\theta}(V_R, \theta)$ be the joint distribution of random velocity magnitudes and directions (as measured from the streaming velocity direction), as computed by equation 23 or, e.g., as a Gaussian velocity whose mean and/or standard deviation is a function of direction. Then, following the same procedure as with equation 24, the resulting velocity magnitudes on the plane of the sky will be distributed as

$$f_{V_{\perp}}(V_{\perp}) = V_{\perp} \int_0^{\pi} \frac{f_{V_R,\theta}(V_R(V_{\perp}, \phi), \theta(V_{\perp}, \phi))}{V_R(V_{\perp}, \phi)} d\phi , \quad (25)$$

where

$$\begin{aligned} V_R(V_\perp, \phi) &= [V_S^2 + V_\perp^2 - 2V_S V_\perp \cos \phi]^{1/2}, \\ \sin(\theta(V_\perp, \phi)) &= \frac{V_\perp \sin \phi}{V_R(V_\perp, \phi)}, \end{aligned}$$

and $V_\perp/V_R(V_\perp, \phi)$ is the Jacobian of the variable transformation from (V_R, θ) to (V_\perp, ϕ) . If the random component is isotropic, this reduces to the relatively simple expression

$$f_{V_\perp}(V_\perp) = \frac{2V_\perp}{\pi} \int_{|V_S - V_\perp|}^{V_S + V_\perp} \frac{f_{V_R}(V_R)}{\sqrt{(2V_S V_\perp)^2 - (V_S^2 + V_\perp^2 - V_R^2)^2}} dV_R. \quad (26)$$

An example may be seen in Figure 4. This rather unusual function has been verified by Monte Carlo simulations independent of the statistical reasoning underlying this derivation. If $V_S \rightarrow 0$ this expression reduces to $f_{V_\perp} = f_{V_R}$, as it must.

C DISTANCE DISTRIBUTION

If the spatial number density of stars varies with galactocentric distance R as $\rho(R)$, and the distribution is radially symmetric about the point from which R is measured, the linear density (number per unit change in R) is easily seen to be $f_R(R) \propto R^2 \rho(R)$. But viewed from off-center, or if the spatial distribution is not radially symmetric, the matter is complicated by the dependence of the density upon the viewing direction. In the case of microlenses viewed against the LMC, the field of view is considerable and it is not obvious how the spatial number density will translate into a linear density in solarcentric distance D when viewed from our off-center position. Formally the solution is straightforward: by the usual change of variables,

$$f_{D,b,l}(D, b, l) \propto R^2 \rho(R) \left| \frac{\partial(R, \phi, \theta)}{\partial(D, b, l)} \right|, \quad (27)$$

where $R = [R_\odot^2 + D^2 - 2R_\odot D \cos b \cos l]^{1/2}$ and (ϕ, θ) are the galactocentric angular coordinates for which we presume connecting relations with the solarcentric position (e.g, $\sin \theta = D \sin b / R(D, b, l)$, etc.). The average value for the field of view is just the integral of this density over the corresponding spreads in b and l . The Jacobian of this relation is difficult to represent analytically, but is numerically trivial. As the field of view shrinks the spatial density becomes more uniform over that field until, in the limit of a small field of view, the solarcentric distance pdf becomes very nearly

$$f_{D,b,l}(D, b, l) \propto D^2 \cdot \rho(R(D, b, l)), \quad (28)$$

where (b, l) refer to the center of the field. In numerical experiments for the LMC direction, with a $\sim 10^0$ wide field and an NFW spatial density profile (cf. §3.2), this approximation agrees with the more exact result (eq. [27]) to within better than 1%, when integrated over the field.

References

- [1] Alcock, C. et al. 1996, *Astrophys.J.*, 461, 82
- [2] Alcock, C. et al. 1997, *Astrophys.J.*, 486, 697
- [3] Alcock, C. et al. 2000, *Astrophys.J.*, 542, 281
- [4] Binney, J. & Tremaine, S. 1987, *Galactic Dynamics* (Princeton: Princeton Univ. Press)
- [5] Binney, J. & Merrifield, M. 1998, *Galactic Astronomy* (Princeton: Princeton Univ. Press)
- [6] Chandrasekhar, S. & Münch, G. 1950, *Astrophys.J.*, 111, 142
- [7] Gould, A. 1996, *Pub.Astron.Soc.Pacific*, 108, 465
- [8] Green, A. M. 2000, *Astrophys.J.*, 537, 708
- [9] Heacock, W. D. 1998, *Astron.J.*, 115, 325
- [10] Heggie, D. & Hut, P. 2003, *The Gravitational Million-Body Problem* (New York: Cambridge Univ. Press)
- [11] Jones, B.F., Klemola, A.R., & Lin, D.N.C. 1994, *Astron.J.*, 107, 1333
- [12] Kendall, M., Stuart, A., & Ord, J.K. 1987, *Kendall's Advanced Theory of Statistics*, Vol. 1, 5th Ed. (New York: Oxford Univ. Press)
- [13] Lucy, L.B. 1974, *Astron.J.*, 79, 745
- [14] Milsztajn, A. et al. 2001, *Nucl. Phys. B. (Proc. Suppl.)*, 91, 413
- [15] Navarro, J.F., Frank, C.S., & White, S.D.M. 1997, *Astrophys.J.*, 490, 493
- [16] Paczyński, R. 1986, *Astrophys.J.*, 304, 1
- [17] Paczyński, R. 1996, *Ann.Rev.Astron.Astrophys.*, 34, 419
- [18] Richardson, W.H. 1972, *J.Opt.Soc.Amer.*, 62,55
- [19] Scheffler, H. & Elsässer, H. 1988, *Physics of the Galaxy and Interstellar Matter* (Berlin: Springer-Verlag)
- [20] Sommer-Larsen, J., Beers, T. C., Flynn, C., Wilhelm, R. & Christensen, P.R. 1997, *Astrophys.J.*, 481, 1997
- [21] Udalski, A. et al. 2000, *Acta Astron.*, 50, 1